Hindawi Publishing Corporation
Journal of Nanomaterials
Volume 2015, Article ID 212493, 7 pages
http://dx.doi.org/10.1155/2015/212493

Research Article

Influence of the Surfactant Nature on the Occurrence of Self-Assembly between Rubber Particles and Thermally Reduced Graphite Oxide during the Preparation of Natural Rubber Nanocomposites

Héctor Aguilar-Bolados,[1] Mehrdad Yazdani-Pedram,[1] Justo Brasero,[2] and Miguel A. Lopez-Manchado[2]

[1]*Faculty of Chemical and Pharmaceutical Sciences, Universidad de Chile, S. Livingstone 1007, 8380492 Santiago, Chile*
[2]*Institute of Polymer Science and Technology, CSIC, Juan de la Cierva 3, 28006 Madrid, Spain*

Correspondence should be addressed to Héctor Aguilar-Bolados; h.aguilar.bolados@gmail.com and Mehrdad Yazdani-Pedram; myazdani@ciq.uchile.cl

Received 4 August 2015; Accepted 17 September 2015

Academic Editor: Stefano Bellucci

The natural rubber (NR) latex consists of polymer particles charged negatively due to the adsorbed phospholipids and proteins molecules. The addition of stable aqueous suspension of thermally reduced graphite oxide (TRGO) stabilized by ionic surfactants to NR latex can favor the occurrence of interaction between the stabilized TRGO and NR particles. Herein, the use of two surfactants of different nature, namely, sodium dodecyl sulfate (SDS) and dodecyltrimethylammonium bromide (DTAB), for the preparation of (TRGO)/NR nanocomposites, is reported. Zeta potential and particle size measurements indicated that the use of DTAB as cationic surfactant results in the flocculation of NR particles and promoted the formation of ion-pair interactions between TRGO and the proteins and/or phospholipids present on the NR surface. This indicates that the use of DTAB can promote a self-assembly phenomenon between TRGO with adsorbed DTAB molecules and NR particles. The occurrence of self-assembly phenomenon allows obtaining homogenous dispersion of TRGO particles in the polymer matrix. The TRGO/NR nanocomposites prepared by the use of DTAB exhibited superior mechanical properties and excellent electrical conductivities reaching values of stress at 500% strain of 3.02 MPa and 10^{-4} S/cm, respectively.

1. Introduction

The use of graphene materials derived from graphite such as thermally reduced graphite oxide (TRGO) as filler in the production of polymer nanocomposites has become an attractive alternative to achieve superior physical and/or mechanical properties [1]. The multiple graphene layers stacked together which are present in the graphite are successfully exfoliated by oxidation and subsequent thermal reduction process. This process allows the TRGO sheets to have greater surface area in contact with the polymer matrix allowing TRGO sheets homogenous dispersion. This results in the formation of a nanofiller network, which could favor the increase of the mechanical and electrical properties of the nanocomposite [2].

Few interesting studies have already been reported illustrating the potential of graphene nanocomposites based on natural rubber (NR) matrices [3–10]. NR nanocomposites can be prepared by different methods such as the use of two-roll mill or by latex technology. The comparative advantage of the use of NR latex to achieve a homogeneous dispersion of TRGO in the polymer matrix has been demonstrated [11].

NR latex is an aqueous colloidal suspension of cis-1,4-polyisoprene particles which is stable due to the presence of proteins and phospholipids adsorbed on the surface of NR particles. Ammonia and other minor additives are usually added to preserve the colloidal stability of the NR latex. Furthermore, these additives hydrolyze the proteins adsorbed on the surface of rubber particles, which further stabilize the colloidal suspension of the NR particles [12]. Although

synthetic surfactants could also be used to further preserve the stability of the NR latex, overuse of surfactants can worsen the mechanical and permeability properties of the NR films [13]. Therefore, the use of surfactants for stabilizing TRGO aqueous suspensions may cause reduction of some properties of TRGO/NR composites. Aguilar-Bolados et al. [6] have reported the use of ionic and nonionic surfactants for the stabilization of aqueous suspensions of TRGO nanoparticles to be used for the preparation of TRGO/NR nanocomposites. The results showed that an anionic surfactant such as sodium dodecyl sulfate (SDS) had a better performance to increase the electrical conductivity of TRGO/NR composites. The addition of TRGO stabilized by SDS to NR latex involves not only the interaction between NR and TRGO but also the interaction between NR and SDS. It has been reported that the colloidal stability of NR latex is not affected at low SDS concentration since its hydrophilic head is oriented toward the aqueous medium in the latex system. This increases the electrical charge of the surface of the latex particles, thus providing greater stability to the system [14]. However, at high SDS concentrations undesirable effects on the interaction of TRGO with NR could occur since SDS induces a repulsion mechanism between NR particles and TRGO, where the TRGO sheets remain occluded between NR particles [15]. This could adversely affect the homogeneous dispersion of the filler particles in the polymer matrix.

Therefore, in this work the use of a cationic surfactant to stabilize the aqueous suspension of TRGO particles, prepared from natural graphite by the method of Brodie [6, 10, 16], was studied. The use of a cationic surfactant such as DTAB could promote interactions between the rubber particles and TRGO sheets, favoring a more homogeneous dispersion of the TRGO in the rubber matrix compared to that achieved by the use of SDS, an anionic surfactant. Moreover, the effect of the surfactant concentration on the stability of TRGO suspension and on mechanical and electrical properties of TRGO/NR nanocomposites was studied. The critical micelle concentration of the surfactant was considered as criterion for the preparation of TRGO suspensions and nanocomposites [17].

2. Experimental

2.1. Materials. Thermally reduced graphite oxide (TRGO) was obtained by thermal reduction of graphite oxide prepared from natural graphite. Glycine and sodium hydroxide of analytical grade from Merck were used for the preparation of a glycine-NaOH buffer solution adjusted to pH 12. The surfactants used to stabilize TRGO in aqueous suspension were sodium dodecyl sulfate (>99%, Fluka) and dodecyltrimethylammonium bromide (>97%, Merck). The prevulcanized natural rubber with 63% of dry rubber content was provided by Química Miralles SA, Chile.

2.2. Preparation and Characterization of Nanocomposites. Aqueous suspensions of TRGO (0.3 wt.%) were prepared by using SDS or DTAB solutions of different concentrations. These suspensions were sonicated at room temperature to obtain stable TRGO dispersion. The critical micelle concentration (CMC) of the surfactant was considered as criteria for the preparation of surfactant solutions, where surfactant concentrations equivalent to $0.5 * \text{CMC}$, $1.0 * \text{CMC}$, and $1.5 * \text{CMC}$ were used for the preparation of aqueous suspensions of TRGO. CMC values at room temperature for SDS and DTAB are 8.20 mM and 15.0 mM, respectively. These TRGO suspensions were then added to the prevulcanized natural rubber latex to obtain nanocomposites containing 3.0 wt.% of TRGO. Moreover, mixtures of NR latex and surfactant solutions of different concentrations were prepared as control samples. All surfactant/NR and surfactant/TRGO/NR samples were dried at 70°C during 12 h to obtain nanocomposite films.

The particle size and Zeta potential of NR latex as well as mixture of surfactant/NR latex and that of TRGO stabilized by surfactant/NR latex were measured at room temperature using Zetasizer Nano series equipment from Malvern Instrument Ltd. The TRGO suspension stabilized by surfactant was sonicated before mixing to the NR latex. The measurement was performed by adding one drop of NR latex to 20 mL of glycine-NaOH buffer solution adjusted to pH 12. The buffer was prepared by mixing 25 mL of 0.2 M glycine solution, 40 mL of 0.2 M sodium hydroxide, and 35 mL of distilled water.

Low temperature scanning electron microscopy (LTSEM) was performed in a DSM 960 Zeiss microscope at −150°C and 15 keV. The samples were mounted on a gold specimen holder using an OCT compound (Tissue, Tek, Sakura, USA) as adhesive. The holder was submerged in nitrogen slush at −210°C, under vacuum. Immediately, the sample was transferred to CT1500 Oxford preparation unit, where the sample was fractured at −170°C. Then, the sample was lyophilized at −90°C in order to eliminate the adsorbed water on the fractured sample surface. Then, the fractured surface was coated with gold by sputtering during 2 minutes at 2 mA and 200 V. The degree of dispersion of the TRGO in the polymeric matrix was measured by transmission electron microscopy by using a Philips Tecnai 20 microscope at an accelerating voltage of 200 kV. Ultrathin sections of the samples were prepared by cryoultramicrotomy at −140°C using a Leica EM UC6 cryoultramicrotome equipment.

The tensile mechanical properties of samples were measured according to the ASTM D 412 norm in an Instron dynamometer model 3366, a crosshead of 500 mm·min^{-1}. The thickness and width of the test specimens were 0.2 mm and 4 mm, respectively, with jaws separation of 4 cm. Five specimens of each sample were tested. The electric conductivity and dielectric permittivity of nanocomposites were measured in a high resolution dielectric spectrometer (Novocontrol Technology, GmbH). The samples with thickness and diameter of 0.2 mm and 10 mm were put between two parallel gold electrodes. The measuring was at room temperature, using 1 V of amplitude of the alternating electrical current, and the frequency range of the measurements was between 10^1 Hz and 10^7 Hz. The electric conductivity of nanocomposites is given by

$$\sigma(\omega) = \sigma_{dc} + A\omega^x, \quad (1)$$

where σ_{dc} is the electric conductivity at direct current, A is a constant, and x is an exponent that describes the dependence

Table 1: Zeta potential distribution of NR latex and mixture of NR latex/SDS, NR latex/DTAB, NR latex/TRGO/SDS, and NR latex/TRGO/DTAB. The surfactant concentrations were 0.5 ∗ CMC, 1.0 ∗ CMC, and 1.5 ∗ CMC.

Sample	Zeta potential (mV)	Z-average (nm)	Peak 1 (nm)	Peak height (%)	Peak width (%)	Peak area (%)	Peak 2 (nm)	Peak height (%)	Peak width (%)	Peak area (%)
NR	−50.3	551,0	327.6	11.6	247.4	100	—	—	—	—
SDS 0.5 ∗ CMC/NR	−56.7	593,9	540.1	4.3	143.9	79.4	154.8	22.8	32.4	79.4
SDS 1.0 ∗ CMC/NR	−56.9	531,8	493.2	3.9	139.7	19.6	158.8	21.9	39.2	80.4
SDS 1.5 ∗ CMC/NR	−60.5	526,6	574.9	2.3	188.4	13.7	168.9	20.2	49.4	86.3
DTAB 0.5 ∗ CMC /NR	−45.3	929,3	729.5	32.2	127.2	100	—	—	—	—
DTAB 1.0 ∗ CMC/NR	−40.0	2736	1005	35.9	170.5	100	—	—	—	—
DTAB 1.5 ∗ CMC/NR	−37.0	3136	1015	33.2	168.8	100	—	—	—	—
SDS 0.5 ∗ CMC/TRGO/NR	−60.2	589	606.6	3.8	157.0	18.1	171.7	22.1	38.1	81.9
SDS 1.0 ∗ CMC/TRGO/NR	−63.7	595,3	502.3	3.9	132	18.2	129.5	25.0	25.4	81.8
SDS 1.5 ∗ CMC/TRGO/NR	−64.1	647	460.1	3.5	129.6	17.6	100.3	24.9	19.5	88.4
DTAB 0.5 ∗ CMC/TRGO/NR	−42.9	2768	836.5	35.1	135.0	100	—	—	—	—
DTAB 1.0 ∗ CMC/TRGO/NR	−40.6	2909	1005	33.6	167.3	100	—	—	—	—
DTAB 1.5 ∗ CMC/TRGO/NR	−34.6	3468	1288	37.5	189.7	100	—	—	—	—

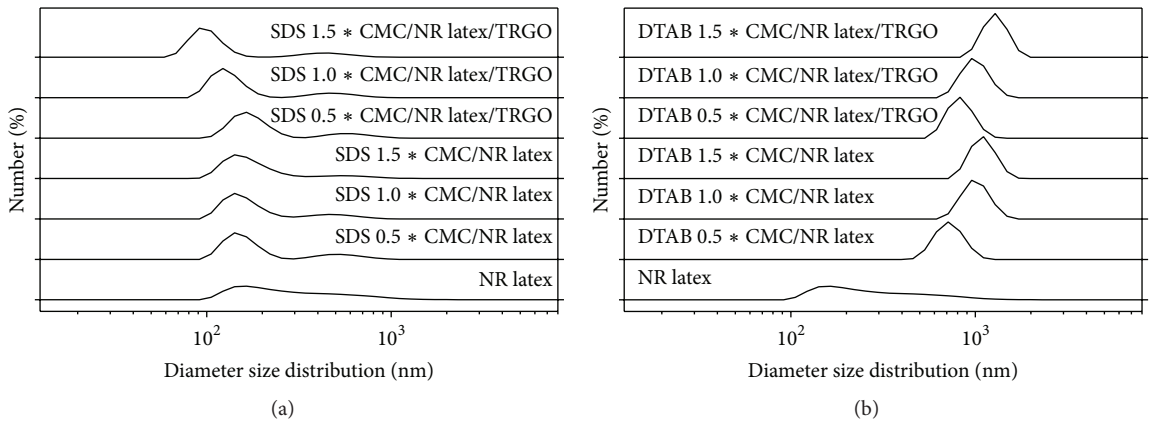

Figure 1: Particle size distribution of NR latex, NR/SDS mixture, and NR latex/TRGO/SDS mixture (a); NR latex, NR latex/DTAB mixtures, and latex/TRGO/DTAB mixtures (b), where the surfactant concentrations were 0.5 ∗ CMC, 1.0 ∗ CMC, and 1.5 ∗ CMC.

of $\sigma(\omega)$ on the frequency (ω). The dielectric responses were evaluated by measuring the complex permittivity ($\varepsilon^*(\omega)$) with respect to the frequency:

$$\varepsilon^*(\omega) = \varepsilon'(\omega) + j\varepsilon''(\omega), \quad (2)$$

where $\varepsilon'(\omega)$ and $\varepsilon''(\omega)$ correspond to the real and imaginary dielectric permittivity, respectively.

3. Results and Discussions

3.1. Determination of Particle Size and Zeta Potential of NR Latex. Figure 1 shows the results of particle size analysis carried out by dynamic light scattering for NR latex, mixture of NR latex and surfactant, and mixture of TRGO stabilized by surfactant/NR latex. Figure 1(a) shows the results obtained when SDS was used, while Figure 1(b) displays the results when DTAB was used as surfactant, respectively. Table 1 shows the Zeta potential for all samples. This value is used to predict the stability of colloids such as NR rubber latex when simple electrolytes are added. NR latex has a Zeta potential value of −50.3 mV; an increase or decrease of this value indicates coalescence or repulsion among the rubber particles. It is observed that the presence of SDS and SDS/TRGO affects the size distribution of NR particles. An increase in the population of particles with lower diameter is observed as a consequence of the disaggregation of NR particles. This could be attributed to the fact that an anionic surfactant such as SDS increases the repulsion among the NR particles that are present as small aggregates in the absence of SDS. This is supported by the values of the Zeta potential which decreases with increasing SDS concentration (Table 1). The decreasing of Zeta potential indicates an increase of the repulsion among the negatively charged NR particles, therefore increasing the colloidal stability of NR latex. When TRGO suspension stabilized by SDS is added to the NR latex, the presence of SDS could weaken the interactions among the TRGO decorated with SDS and NR particles. On the other hand, NR

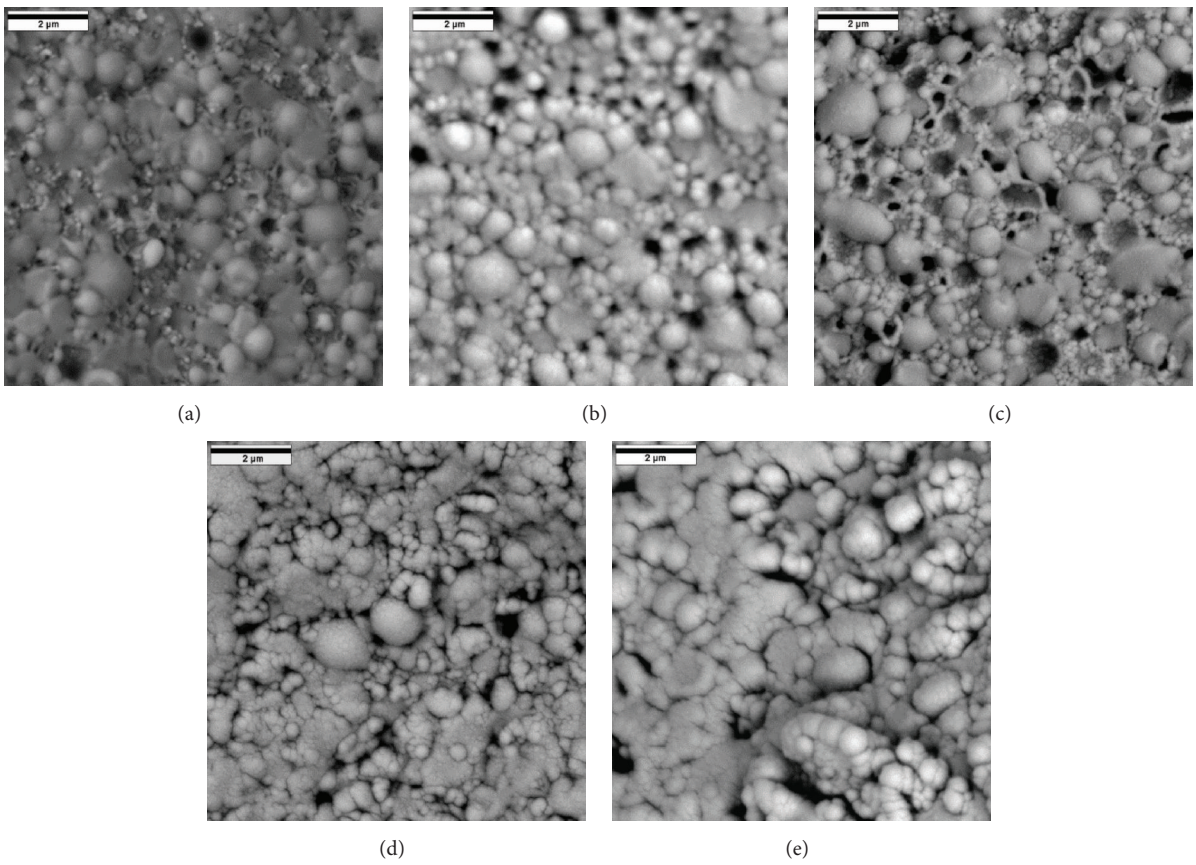

Figure 2: Low temperature scanning electron microscopy images of NR (a), SDS 1.5 ∗ CMC/NR (b), DTAB 1.5 ∗ CMC/NR (c), SDS 1.5 ∗ CMC/TRGO/NR (d), and DTAB 1.5 ∗ CMC/TRGO/NR (e).

latex samples containing DTAB exhibit only one peak in the size distribution analysis. These peaks represent NR particles with larger diameter suggesting that the presence of DTAB favors the flocculation of NR particles. This was confirmed by Zeta potential results. As the content of DTAB is increased, the Zeta potential values increase. This could indicate that the DTAB molecules tend to interact with phospholipids or proteins present on the surface of NR particles, forming a possible ion-pair type interaction between DTAB and the surface of NR. Therefore, the interaction between TRGO decorated with DTAB molecules and NR particles surface is improved, thereby favoring a self-assembly between NR particles and DTAB/TRGO.

3.2. Morphology of TRGO/NR Nanocomposites. Figure 2 displays images of low temperature scanning electron microscopy (LTSEM) of NR, NR and SDS or NR and DTAB mixtures, and NR nanocomposites with TRGO dispersed in either SDS or DTAB. The morphology exhibited by samples is similar, indicating that the presence of surfactant does not affect the NR film formation process [15]. DTAB/TRGO/NR nanocomposite shows apparently a greater aggregation of NR particles presenting a more homogeneous particle size distribution than SDS/TRGO/NR nanocomposite. This indicates that NR could induce self-assembly of TRGO flakes and NR particles.

Figure 3 shows TEM analysis of nanocomposites. Low electronic density areas observed correspond to NR particles, while areas with higher electron density around these areas correspond to TRGO. This indicates that the TRGO sheets are occluded by rubber particles. TRGO dispersed in SDS show a higher tendency to form aggregates resulting in less interaction with NR particles. However, in the case of DTAB/TRGO/NR nanocomposites, the TRGO sheets show a more homogeneous distribution in the NR matrix indicating better interaction with the rubber particles.

3.3. Mechanical Properties on TRGO/NR Nanocomposites. The mechanical properties of TRGO/NR nanocomposites by using TRGO dispersed in SDS or DTAB are shown in Table 2. It is observed that TRGO/NR nanocomposites prepared by using TRGO dispersed in DTAB at a concentration of 0.5 ∗ CMC and 1.0 ∗ CMC exhibit slightly lower values of mechanical properties compared with NR. The decreasing of stress at 100% strain of nanocomposites could be attributed to the plasticizing effect of DTAB due to the interaction of DTAB with NR particles [6, 13]. The slight decrease of tensile strength of DTAB/TRGO/NR nanocomposites with low DTAB content (DTAB 0.5 ∗ CMC/TRGO (3 wt.%)/NR and DTAB 1.0 ∗ CMC/TRGO (3 wt.%)/NR) could be attributed to the poor dispersion of TRGO achieved by using these surfactant/TRGO ratios. Nevertheless, increasing the DTAB concentration to 1.5 ∗ CMC allows achieving higher stress at 100% strain compared with that of NR. This suggests that TRGO achieves a homogenous dispersion in the polymeric

Table 2: Mechanical properties of nanocomposites of NR and TRGO (3 wt.%) dispersed in DTAB or SDS. Surfactant concentrations were 0.5 ∗ CMC, 1.0 ∗ CMC, and 1.5 ∗ CMC.

Sample	Stress at 100% strain (MPa)	Stress at 300% strain (MPa)	Stress at 500% strain (MPa)	Maximum stress (MPa)	Deformation at break (%)
NR	0.49 ± 0.01	0.83 ± 0.02	1.39 ± 0.10	13.99 ± 1.01	892 ± 6
SDS 0.5 ∗ CMC/TRGO (3 wt.%)/NR	0.49 ± 0.02	1.04 ± 0.03	2.22 ± 0.17	4.55 ± 0.20	640 ± 26
SDS 1.0 ∗ CMC/TRGO (3 wt.%)/NR	0.47 ± 0.1	0.98 ± 0.06	2.23 ± 0.13	8.67 ± 0.68	837 ± 48
SDS 1.5 ∗ CMC/TRGO (3 wt.%)/NR	0.56 ± 0.02	0.91 ± 0.02	1.73 ± 0.06	7.04 ± 0.69	792 ± 78
DTAB 0.5 ∗ CMC/TRGO (3 wt.%)/NR	0.43 ± 0.02	0.89 ± 0.01	1.68 ± 0.04	4.45 ± 0.36	759 ± 50
DTAB 1.0 ∗ CMC/TRGO (3 wt.%)/NR	0.40 ± 0.02	0.89 ± 0.01	1.69 ± 0.03	4.61 ± 0.13	788 ± 40
DTAB 1.5 ∗ CMC/TRGO (3 wt.%)/NR	0.65 ± 0.01	1.28 ± 0.02	3.02 ± 0.07	15.14 ± 1.04	806 ± 23

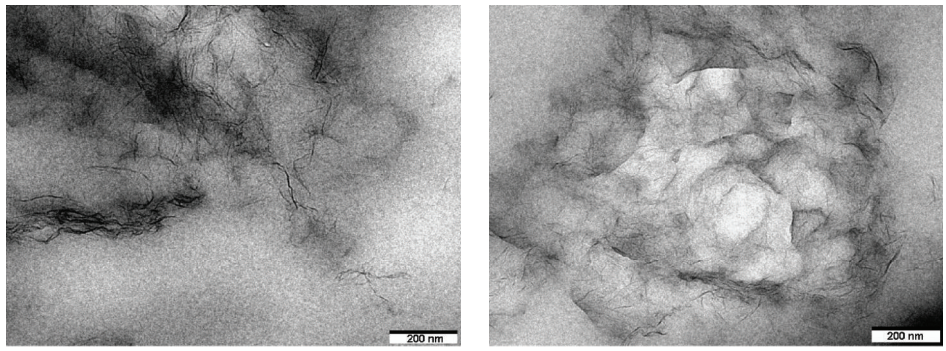

(a) (b)

Figure 3: TEM images of nanocomposites of SDS 1.5 ∗ CMC/TRGO/NR (a) and DTAB 1.5 ∗ CMC/TRGO/NR (b).

matrix when it is dispersed in surfactant solution with a concentration higher than CMC. A similar effect is observed for SDS 1.5 ∗ CMC/TRGO/NR composite. This composite shows slightly higher stress values at 100%, 300%, and 500% strain than NR, which could be related to a more homogeneous dispersion of TGRO in the rubber matrix. However, the decrease of maximum stress can be related to high SDS content in the nanocomposite, which could produce SDS domains as defects in the nanocomposite film [6].

3.4. Electrical Properties of TRGO/NR Nanocomposites. Figure 4 shows the dielectric spectroscopy of NR nanocomposites with TRGO dispersed in SDS (Figures 4(a) and 4(b)) or DTAB (Figures 4(c) and 4(d)), where the electrical conductivity and dielectric permittivity, as function of frequency, are shown. DTAB/TRGO/NR nanocomposites exhibit a significant increase in the electrical conductivity and dielectric permittivity with increased surfactant content as compared to NR. SDS/TRGO/NR nanocomposites do not show a marked improvement of the NR properties but maintain the tendency to increase the electrical conductivity and dielectric permittivity of the material with increasing surfactant content. This could indicate that the dispersion of TRGO in the polymer matrix is favored by increasing content of surfactants. This is due to the higher number of Van der Waals type interactions between TRGO and the hydrophobic tails of surfactants in the aqueous medium. The nanocomposites with higher electrical conductivity show two zones, at low frequencies, a frequency independent zone or ohmic zone and a second zone at higher frequencies, where capacitance effects are important. Although ohmic zone is partially present in SDS 1.5 ∗ CMC/TRGO/NR and DTAB 0.5 ∗ CMC/TRGO/NR, the change in conductivity is small as compared with DTAB 1.0 ∗ CMC/TRGO/NR and DTAB 1.5 ∗ CMC/TRGO/NR nanocomposites, where the frequency independent zone appears in almost all window of frequency analyzed. This is complemented with the negative slope they present for the dielectric permittivity. This effect has been related to the Maxwell-Wagner-Sillars effect, which consists in the interface polarization of insulating polymer/conductive filler for heterophasic systems [18, 19].

The ability of TRGO for promoting the formation of an effective electrical percolation network when DTAB was used is evidenced by comparing the electrical properties of the resulting nanocomposites prepared by using this surfactant compared with those prepared with SDS. This indicates that DTAB promotes the self-assembly between NR and TRGO nanoparticles and consequently a homogeneous dispersion of TRGO through the polymer matrix was favored (Figure 5). This indicates that the nature of surfactant plays a crucial role to obtain TRGO/NR nanocomposites with higher electrical conductivities. It is worth mentioning that the proposed scheme in Figure 5 clearly shows the arrangement of TRGO layers in the interstices of NR particles evidencing the possible interactions between polar heads of DTAB with phospholipids and proteins present on the surface of NR particles.

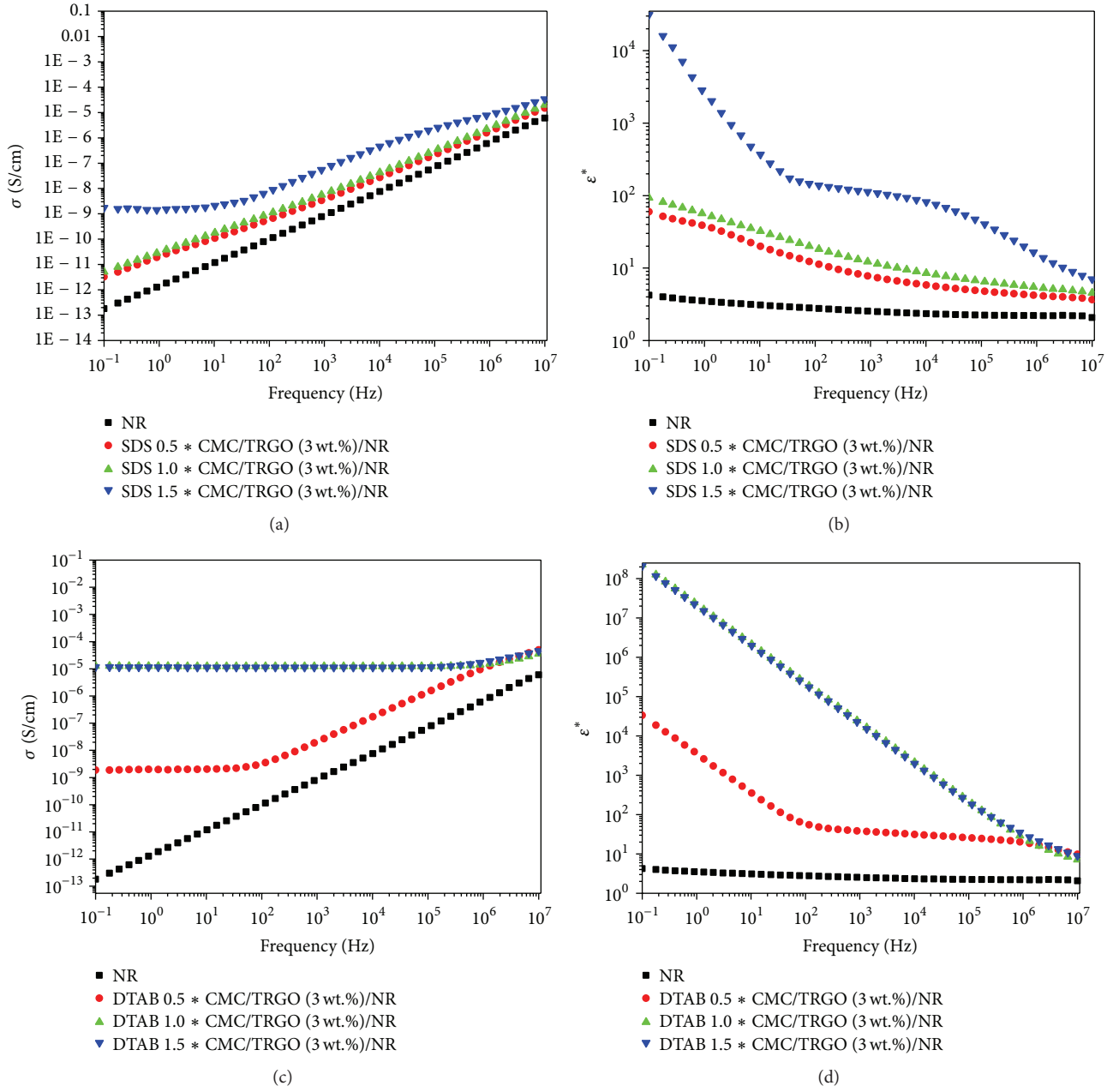

Figure 4: Electrical conductivity and dielectric permittivity of SDS/TRGO (3 wt.%)/NR nanocomposites (a and b) or DTAB/TRGO (3 wt.%)/NR (c and d). The surfactant concentrations were 0.5 ∗ CMC, 1.0 ∗ CMC, and 1.5 ∗ CMC.

4. Conclusions

It is demonstrated that the nature of the ionic surfactant affects the colloidal stability of NR latex through particle size and Zeta potential analyses. Although SDS improves the colloidal stability of NR latex by decreasing the Zeta potential and disaggregation of NR particles, DTAB promotes a slight flocculation of NR particles. Consequently, the Zeta potential values increase resulting in an increment of the number of NR particles with larger diameter. Therefore, the change observed for NR latex stability is induced by DTAB. This can be explained by the existence of ionic type interactions between the negatively charged NR particles and positively charged surfactant head. The interaction of TRGO decorated with DTAB and NR particle surface leads to the occurrence of self-assembly phenomenon between NR particles and TRGO particles stabilized by DTAB. This results in a significant increase of the electrical conductivity and mechanical strength of the nanocomposites.

Conflict of Interests

The authors declare that there is no conflict of interests regarding the publication of this paper.

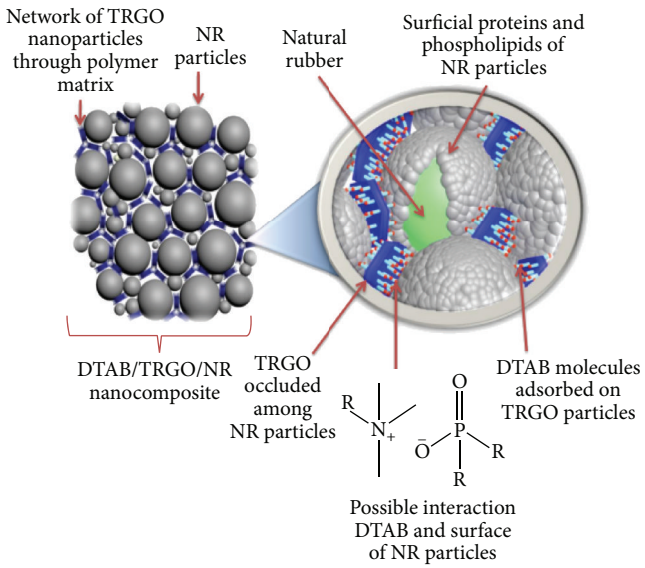

Figure 5: Scheme proposed for self-assembly between the NR and TRGO nanoparticles.

Acknowledgments

This research was supported by National Commission for the Scientific and Technological Research (CONICYT) Project FONDECYT 1131139 and Spanish Ministry of Science and Innovation (MICINN), Spain, under Project MAT 2013-48107-C3-2-R.

References

[1] R. Verdejo, M. M. Bernal, L. J. Romasanta, and M. A. Lopez-Manchado, "Graphene filled polymer nanocomposites," *Journal of Materials Chemistry*, vol. 21, no. 10, pp. 3301–3310, 2011.

[2] M. Tian, J. Zhang, L. Zhang et al., "Graphene encapsulated rubber latex composites with high dielectric constant, low dielectric loss and low percolation threshold," *Journal of Colloid and Interface Science*, vol. 430, pp. 249–256, 2014.

[3] J. R. Potts, O. Shankar, L. Du, and R. S. Ruoff, "Processing-morphology-property relationships and composite theory analysis of reduced graphene oxide/natural rubber nanocomposites," *Macromolecules*, vol. 45, no. 15, pp. 6045–6055, 2012.

[4] M. Hernández, M. D. M. Bernal, R. Verdejo, T. A. Ezquerra, and M. A. López-Manchado, "Overall performance of natural rubber/graphene nanocomposites," *Composites Science and Technology*, vol. 73, no. 1, pp. 40–46, 2012.

[5] Y. Zhan, M. Lavorgna, G. Buonocore, and H. Xia, "Enhancing electrical conductivity of rubber composites by constructing interconnected network of self-assembled graphene with latex mixing," *Journal of Materials Chemistry*, vol. 22, no. 21, pp. 10464–10468, 2012.

[6] H. Aguilar-Bolados, J. Brasero, M. A. Lopez-Manchado, and M. Yazdani-Pedram, "High performance natural rubber/thermally reduced graphite oxide nanocomposites by latex technology," *Composites Part B: Engineering*, vol. 67, pp. 449–454, 2014.

[7] D. C. Stanier, A. J. Patil, C. Sriwong, S. S. Rahatekar, and J. Ciambella, "The reinforcement effect of exfoliated graphene oxide nanoplatelets on the mechanical and viscoelastic properties of natural rubber," *Composites Science and Technology*, vol. 95, pp. 59–66, 2014.

[8] G. Scherillo, M. Lavorgna, G. G. Buonocore et al., "Tailoring assembly of reduced graphene oxide nanosheets to control gas barrier properties of natural rubber nanocomposites," *ACS Applied Materials and Interfaces*, vol. 6, no. 4, pp. 2230–2234, 2014.

[9] N. Yan, G. Buonocore, M. Lavorgna et al., "The role of reduced graphene oxide on chemical, mechanical and barrier properties of natural rubber composites," *Composites Science and Technology*, vol. 102, pp. 74–81, 2014.

[10] H. Aguilar-Bolados, M. A. Lopez-Manchado, J. Brasero, F. Avilés, and M. Yazdani-Pedram, "Effect of the morphology of thermally reduced graphite oxide on the mechanical and electrical properties of natural rubber nanocomposites," *Composites Part B: Engineering*, 2015.

[11] J. R. Potts, O. Shankar, S. Murali, L. Du, and R. S. Ruoff, "Latex and two-roll mill processing of thermally-exfoliated graphite oxide/natural rubber nanocomposites," *Composites Science and Technology*, vol. 74, pp. 166–172, 2013.

[12] H. Alenius and T. Palosuo, "Allergenic proteins," in *Latex Intolerance: Basic Science, Epidemiology, and Clinical Management*, M. M. U. Chowdhury, Ed., pp. 15–26, CRC Press, Boca Raton, Fla, USA, 2005.

[13] P. A. Steward, J. Hearn, and M. C. Wilkinson, "An overview of polymer latex film formation and properties," *Advances in Colloid and Interface Science*, vol. 86, no. 3, pp. 195–267, 2000.

[14] K. Nawamawat, J. T. Sakdapipanich, and C. C. Ho, "Effect of deproteinized methods on the proteins and properties of natural rubber latex during storage," *Macromolecular Symposia*, vol. 288, no. 1, pp. 95–103, 2010.

[15] J. L. Keddie and A. F. Routh, *Fundamentals of Latex Film Formation—Processes and Properties*, Springer, Dordrecht, The Netherlands, 2010.

[16] B. C. Brodie, "On the atomic weight of graphite," *Philosophical Transactions of the Royal Society of London*, vol. 149, pp. 249–259, 1859.

[17] J. Aguiar, P. Carpena, J. A. Molina-Bolívar, and C. Carnero Ruiz, "On the determination of the critical micelle concentration by the pyrene 1:3 ratio method," *Journal of Colloid and Interface Science*, vol. 258, no. 1, pp. 116–122, 2003.

[18] M. Martin-Gallego, M. Hernández, V. Lorenzo, R. Verdejo, M. A. Lopez-Manchado, and M. Sangermano, "Cationic photocured epoxy nanocomposites filled with different carbon fillers," *Polymer*, vol. 53, no. 9, pp. 1831–1838, 2012.

[19] D. Hayward, R. A. Pethrick, and T. Siriwittayakorn, "Dielectric studies of heterogeneous phase polymer systems: poly(ethylene oxide) inclusions in polycarbonate—a model system," *Macromolecules*, vol. 25, no. 5, pp. 1480–1486, 1992.